Kinetic Modeling of the Effect of H_2S and of NH_3 on Toluene Hydrogenation in the Presence of a $NiMo/Al_2O_3$ Hydrotreating Catalyst. Discrimination between Homolytic and Heterolytic Models

S. Blanchin,[†] P. Galtier,[‡] S. Kasztelan,[§] S. Kressmann,[‡] H. Penet,[†,||] and G. Pérot*[,†]

Laboratoire de Catalyse en Chimie organique, Faculté des Sciences de l'Université de Poitiers, 40 avenue du recteur Pineau, 86022 Poitiers Cedex, France, Institut Français du Pétrole Solaize, BP 3, 69390 Vernaison, France, and Institut Français du Pétrole, 1 et 4 avenue de bois préau, 92852 Rueil-Malmaison Cedex, France

Received: April 10, 2001; In Final Form: July 25, 2001

Toluene hydrogenation was studied within a wide range of hydrogen sulfide, hydrogen, toluene, and ammonia partial pressures on a standard sulfided $NiMo/Al_2O_3$ hydrotreating catalyst at 350 °C under a total pressure of 4.9−9.8 MPa. The results showed a complex inhibiting effect of H_2S on the hydrogenation activity with an order of reaction relative to H_2S varying between −0.05 and −0.5. Unexpectedly, this inhibiting effect was enhanced by the presence of ammonia. Several kinetic models based on the homolytic or heterolytic dissociation of hydrogen and hydrogen sulfide were investigated and discriminated by using the CHEMKIN/SURFACE CHEMKIN II tool. The heterolytic dissociation was supposed to occur on centers composed of an unsaturated Mo ion (on which hydride ions and organic molecules can adsorb) and of a sulfur anion, host of the proton generated by the heterolytic dissociation of hydrogen or hydrogen sulfide. It was concluded that toluene hydrogenation was most likely to occur through a heterolytic mechanism starting with a hydride addition followed by a proton addition. In the range of H_2S partial pressures investigated, the latter was the rate-determining step.

Introduction

Because of more severe pending specifications regarding the concentration of aromatics in diesel fuels, there has been recently a renewed interest in kinetics studies dealing with the hydrogenation of these compounds under hydrotreating conditions. Hydrotreating catalysts work in the presence of H_2S and of NH_3 which are often considered as simple inhibitors due to their competitive adsorption with unsaturated hydrocarbons as well as with S and N heterocompounds. However, studies in a wide range of partial pressures showed that H_2S had an effect which was more complex than a simple inhibition of hydrogenation reactions.[1] This was also the case with hydrodenitrogenation where H_2S was found to have both a promoting effect (at low H_2S partial pressure) and an inhibiting effect (at high H_2S partial pressure).[2−5] A certain lack of knowledge regarding all the elementary steps involved in the reaction and their mechanism can explain the difficulties in representing a general picture of the kinetics of hydrotreating reactions and more specifically in quantifying the effect of H_2S and of NH_3. A better understanding of these effects is essential to extend the kinetic modeling to industrial feedstocks.

In the recent years, new models based on the dissociation of hydrogen and of hydrogen sulfide have been introduced to explain the complex effect of H_2S. In particular, the heterolytic dissociation of hydrogen and of hydrogen sulfide was considered and seemed to account for the H_2S kinetic order in the hydrogenation of toluene on a MoS_2/Al_2O_3 catalyst.[1] Several authors[6−11] have postulated the presence of hydride species produced by the heterolytic dissociation of hydrogen. On RuS_2, Lacroix et al.[12] observed hydride species by NMR, which was confirmed by a neutron diffusion study.[13] Theoretical studies showed that the heterolytic dissociation of hydrogen was also likely to occur on MoS_2.[14] The aim of this work was to investigate by kinetic modeling the hydrogenation of toluene on a sulfided $NiMo/Al_2O_3$ catalyst, to discriminate between homolytic and heterolytic mechanisms and to quantify the effect of H_2S and of NH_3.

Experimental Section and Methods

Materials and Reaction Conditions. *Catalyst.* The catalyst used in this work was a standard $NiMo/Al_2O_3$ catalyst (14 wt % MoO_3 and 3 wt % NiO on a γ-alumina with a BET surface area of 240 m^2/g). It was crushed and screened for particles between 0.25 and 0.315 mm. Prior to use, the catalyst was sulfided in situ by passing a feed containing 4.75 vol % dimethyldisulfide in *n*-heptane (LHSV = 1 h^{-1}) under a hydrogen pressure of 1.5 MPa and a total pressure of 3.5 MPa. The catalyst was heated under hydrogen up to 150 °C; then the sulfiding mixture (dimethyldisulfide in *n*-heptane) was introduced and the temperature raised to 350 °C (2 °C/min with stages of 1 h every 30 °C) for a 12h treatment.

Procedure. The reactions were performed in a continuous flow fixed bed microreactor under pressure. The liquid products were condensed in a gas−liquid separator and analyzed by gas chromatography using a 30 m DB1 column and a flame

* To whom correspondence should be addressed. Fax: (33) 5 49 45 38 99. E-mail: guy.perot@univ-poitiers.fr.

[†] Laboratoire de Catalyse en Chimie organique, Faculté des Sciences de l'Université de Poitiers.

[‡] Institut Français du Pétrole Solaize.

[§] Institut Français du Pétrole.

[||] Present address: Rhodia Recherche, BP 62 85 avenue des frères Perret, 69192 St Fons - France.

10.1021/jp011352a CCC: $20.00
Published on Web 11/08/2001

ionization detector. The column was maintained at 45 °C for 5 min then the temperature was increased at 8 °C/min up to 120 °C.

The experimental conditions were as follows: a total pressure between 4.9 and 9.8 MPa, a reaction temperature of 350 °C, 2.5 cm^3 of catalyst, and a liquid hourly space velocity (LHSV) between 32 and 211 h^{-1}. A series of experiments was carried out to verify that the reaction was not diffusion-limited under our operating conditions. Samples of catalyst of different sizes were used with different reactant space velocities in order to obtain the same contact time for values of the latter between 25 s and 144 s. For a given contact time, the same conversion rates were obtained for different catalyst weights and space velocities, which indicates the absence of extragranular diffusionnal limitations.[15] The Thiele modulus was calculated and found smaller than 0.2, which confirmed that the reaction was not limited by intragranular diffusion. The catalyst efficiency could be estimated by using the value of the Thiele modulus and was found close to unity whatever the conditions.

The effect of the concentration of the various components was studied within a wide range of partial pressures. The liquid feed was composed of toluene (between 12 and 52 vol %), dimethyldisulfide (between 0.3 and 18 vol %) and cyclohexane (between 33 and 78 vol %). Dimethyldisulfide was used as a H_2S precursor. Under the experimental conditions, it was completely converted into methane and H_2S. Under standard conditions, the partial pressures were 5 MPa H_2, 0.4 MPa toluene, 0.1 MPa H_2S, 0.1 MPa methane, and 1.4 MPa cyclohexane corresponding to a liquid feed composition of 21.5 vol % toluene, 2.3 vol % dimethyldisulfide, and 76.2 vol % cyclohexane.

The hydrogenation of toluene was also studied in the presence of ammonia at 350 °C. Butylamine was used as a NH_3 precursor; under the reaction conditions it was completely decomposed into ammonia and butane. The effects of hydrogen, hydrogen sulfide, and toluene were also examined within a wide range of partial pressures in the presence of ammonia. The liquid feed was composed of toluene (between 11 and 35 vol %), dimethyl disulfide (between 0.9 and 7.15 vol %), butylamine (between 0.1 and 2.75 vol %) and cyclohexane (between 59 and 86 vol. %). The total pressure varied between 4.705 and 8.82 MPa and LHSV between 38 and 231 h^{-1}. Under standard conditions, the partial pressure were 5 MPa hydrogen, 0.4 MPa toluene, 0.1 MPa methane and hydrogen sulfide, 0.01 MPa butane and ammonia and 1.4 MPa cyclohexane corresponding to a liquid feed composition of 21.3 vol % toluene, 0.5 vol % dimethyl disulfide, and 2.2 vol % butylamine and 76 vol % cyclohexane.

Kinetic Modeling. *General Approach.* The kinetic models developed in this work consisted in writing all the elementary steps for the hydrogenation of toluene. Several models (homolytic and heterolytic) were considered to account for the results. Two hypotheses were made: the adsorption/desorption steps were assumed to be at equilibrium and the number of active sites was supposed constant. However, the interest of this approach is that it does not require to make the assumptions on the rate-determining step which are necessary in the case of Langmuir−Hinshelwood models. It makes it possible to obtain information on the rate of every elementary step involved in the reaction and to estimate the surface coverage by the adsorbed species. The reaction network was interpreted by using the CHEMKIN/SURFACE-CHEMKIN II code.[16,17] The CHEMKIN/SURFACE-CHEMKIN interpreters are able to read the conventional description of the elementary chemical reactions in gas phase and on solid surfaces. The CHEMKIN/SURFACE-CHEMKIN II code was adapted to calculate the rates of surface reactions which were necessary to solve the differential/algebraic equations of the reactor. Theses equations were resolved by using the DASSL code.[18] The method uses the GEAR's numerical resolution code.[19]

TABLE 1: Reaction Schemes

A. model 1: homolytic model

$CHX + ✱\text{-}V \rightleftharpoons ✱\text{-}CHX$	b_{CHX}
$T + ✱\text{-}V \rightleftharpoons ✱\text{-}T$	b_T
$MCH + ✱\text{-}V \rightleftharpoons ✱\text{-}MCH$	b_{MCH}
$H_2S + 2\ ✱\text{-}V \rightleftharpoons ✱\text{-}SH + ✱\text{-}H$	B_{H_2S}
$H_2 + 2\ ✱\text{-}V \rightleftharpoons 2\ ✱\text{-}H$	B_{H_2}

$$✱\text{-}T + ✱\text{-}H \underset{k_{-1}}{\overset{k_1}{\rightleftharpoons}} ✱\text{-}TH + ✱\text{-}V$$

$$✱\text{-}TH + ✱\text{-}H \underset{k_{-2}}{\overset{k_2}{\rightleftharpoons}} ✱\text{-}TH_2 + ✱\text{-}V$$

$$✱\text{-}TH_2 + 4\ ✱\text{-}H \underset{k_{-3}}{\overset{k_3}{\rightleftharpoons}} ✱\text{-}MCH + 4\ ✱\text{-}V$$

B. heterolytic models

model 2, hydride addition first

$CHX + ✱\text{-}V \rightleftharpoons ✱\text{-}CHX$	b_{CHX}
$T + ✱\text{-}V \rightleftharpoons ✱\text{-}T$	b_T
$MCH + ✱\text{-}V \rightleftharpoons ✱\text{-}MCH$	b_{MCH}
$H_2S + ✱\text{-}V + ●\text{-}S^{2-} \rightleftharpoons ✱\text{-}SH^- + ●\text{-}S^{2-}(H^+)$	B_{H_2S}
$H_2 + ✱\text{-}V + ●\text{-}S^{2-} \rightleftharpoons ✱\text{-}H^- + ●\text{-}S^{2-}(H^+)$	B_{H_2}

$$✱\text{-}T + ✱\text{-}H^- \underset{k_{-1}}{\overset{k_1}{\rightleftharpoons}} ✱\text{-}TH^- + ✱\text{-}V$$

$$✱\text{-}TH^- + ●\text{-}S^{2-}(H^+) \underset{k_{-2}}{\overset{k_2}{\rightleftharpoons}} ✱\text{-}TH_2 + ●\text{-}S^{2-}$$

$$✱\text{-}TH_2 + 2\ ✱\text{-}H^- + 2\ ●\text{-}S^{2-}(H^+) \underset{k_{-3}}{\overset{k_3}{\rightleftharpoons}} ✱\text{-}MCH + 2\ ✱\text{-}V + 2\ ●\text{-}S^{2-}$$

model 3, proton addition first

$$✱\text{-}T + ●\text{-}S^{2-}(H^+) \underset{k_{-1}}{\overset{k_1}{\rightleftharpoons}} ✱\text{-}TH^+ + ●\text{-}S^{2-}$$

$$✱\text{-}TH^+ + ✱\text{-}H^- \underset{k_{-2}}{\overset{k_2}{\rightleftharpoons}} ✱\text{-}TH_2 + ✱\text{-}V$$

$$✱\text{-}TH_2 + 2\ ✱\text{-}H^- + 2\ ●\text{-}S^{2-}(H^+) \underset{k_{-3}}{\overset{k_3}{\rightleftharpoons}} ✱\text{-}MCH + 2\ ✱\text{-}V + 2\ ●\text{-}S^{2-}$$

C. adsorption/desorption equation of ammonia

mode A

$NH_3 + ✱\text{-}V \rightleftharpoons ✱\text{-}NH_3$	b_{NH_3}

mode B

$NH_3 + ●\text{-}S^{2-}(H^+) \rightleftharpoons ●\text{-}S^{2-}(NH_4^+)$	$b_{NH_4^+}$

CHX: Cyclohexane (solvent) T: Toluene MCH: Méthylcyclohexane

Catalytic Reaction Network and Models for Adsorption and Dissociation of the Reactants. Before writing surface reactions, we have to consider the adsorption/desorption of the reactants (hydrogen, hydrogen sulfide, ammonia, toluene), products (methylcyclohexane) and solvent (cyclohexane). In fact, preliminary optimization trials showed that adsorption/desorption steps were much faster than surface reactions. It is the reason we considered that the asdsorption/desorption steps were near equilibrium. For each of them, an adsorption/desorption constant, b_k (cm^3/mol), or B_k (cm^3/mol) for dissociative adsorption, was assigned (see Table 1). The models involve the dissociation of H_2 and H_2S which can be either homolytic or heterolytic.

In the case of the homolytic dissociation that leads to two identical hydrogen species adsorbed on the surface, only one toluene hydrogenation mechanism can be written (Model 1, Table 1A).

The heterolytic dissociation of hydrogen and hydrogen sulfide was considered in the case of sulfide catalysts.[1,20] The heterolytic dissociation can occur on a dual catalytic center composed of a coordinatively unsaturated Mo ion of the surface (✱-V) and a sulfur anion (●-S^{2-}). The heterolytic dissociation of hydrogen

and of hydrogen sulfide produces a proton and a hydride and a proton and a sulfhydril group respectively (see Table 1B). With the heterolytic dissociation, two sequences can be considered depending on the order of the hydrogen species addition to the toluene molecule, hydride first then proton (Model 2, Table 1B) or proton first then hydride (Model 3, Table 1B).

In all the models, the addition of the last four hydrogen species was written globally (Table 1) and was considered to be at equilibrium.

For the reactions with ammonia, equations corresponding to ammonia adsorption/desorption must be added. In the case of the homolytic model, ammonia was supposed to coordinatively adsorb on a coordinatively unsaturated Mo ion (✱-V) giving ✱-NH_3 (Mode A, Table 1C).

In the case of the heterolytic model, two hypotheses can be postulated regarding the adsorption/desorption mode of ammonia:

(i) the coordination of ammonia on a coordinatively unsaturated Mo ion (Mode A, Table 1C);

(ii) the protonation of ammonia by a proton adsorbed on a sulfur anion (●-$S^{2-}(H^+)$) leading to an ammonium ion connected to a sulfur anion, ●-$S^{2-}(NH_4+)$ (Mode B, Table 1C).

Three models were tested regarding the experiments in the presence of ammonia. Models 1 and 2 were combined with the two different models for the adsorption of ammonia (by coordination and by protonation, Table 1C). The heterolytic model with the proton addition first (Model 3) which was found less predictive than the others (see Results and Discussion) was not selected. Model 1A corresponds to Model 1 combined with the ammonia adsorption by coordination (Mode A). Model 2A corresponds to Model 2 combined with ammonia adsorption by coordination (Mode A) and Model 2B corresponds to Model 2 combined with ammonia adsorption by protonation (Mode B).

Reactor Model. The kinetic models were based on the material balance equations. Assuming a plug flow regime, the material balance equation for a component in a gas phase can be written as

$$\frac{\partial Y_k}{\partial t_c} = \dot{S}_k A w_k \frac{\rho_c}{\rho} \qquad k = 1,...,n_g \tag{1}$$

where $\dot{S}_k$ is the rate of production/destruction of the species k. $\dot{S}_k$ is calculated with a CHEMKIN subroutine which calls the vector containing the kinetic constants assigned to each elementary steps.

Two categories of surface species can be distinguished depending on whether they desorb or not. For the species which desorb, the surface coverage Z_k of the species is obtained from the adsorption/desorption equilibrium constant b_k, (B_k for dissociative adsorption/desorption) according to the equation

$$Z_k^n = b_k C_k^{gas} Z_s^n \qquad k = 1,...,n_g \tag{2}$$

For the surface species which do not desorb, the surface coverage of the component k is obtained by resolving the equation

$$\dot{S}_k = 0 \tag{3}$$

This equation means that the rate of production/destruction is null for the species which do not desorb. The surface coverage of each site *n* by adsorbed species is normalized according to the equation

$$\sum_{m(n)} Z_k{}^n = 1 \tag{4}$$

where $m(n)$ is the number of surface species which are adsorbed on the site of type *n*.

The heterolytic model leads to formally electrostatically charged species although this may not correspond to reality. Consequently, an equation for electrostatic charge conservation must be added to avoid the singularity of the systems[21]

$$\sum Z_{k^+} - \sum Z_{k^-} = 0 \tag{5}$$

The mole fraction of each component at the inlet of the reactor is known. However, the initial surface coverages have to be computed. This is done by resolving a transitory system with eq 2 for the species which adsorb and desorb and eq 6 for the species which do not desorb

$$\frac{\partial Z_k^n}{\partial t} = \dot{S}_k \tag{6}$$

The surface coverages are obtained when the differences between the surface coverages calculated at step *t* and at step ($t - 1$) are smaller than the requested tolerance.

This modeling makes it possible to determine the surface coverage and partial pressure for each component at each point of the reactor and it can therefore account for differences in order of reaction with respect to a given compound between the inlet and the outlet of the reactor.

Parameter Estimation. The three models consist of 5 adsorption/desorption reactions and 3 reversible catalytic reactions leading to 9 parameters. Parameter k_3 was assigned because step 3 was considered to be at equilibrium; consequently parameter k_{-3} was determined by using the thermodynamic equilibrium constant *K*p of toluene hydrogenation (eq 7)

$$K_p = \frac{k_1 k_2 k_3}{k_{-1} k_{-2} k_{-3}} \frac{B_{H_2}^3 b_{toluene}}{b_{MCH}} * \left(\frac{P}{RT}\right)^3 \tag{7}$$

All the parameters were optimized by using the GRG minimization algorithm for nonlinear constraints.[22] The parameter estimates were obtained by minimization of the least-squares functions (objective function) applied to the difference between the calculated ($\hat{x}_i$) and the experimental (x_i) conversion of toluene at the reactor outlet

$$S = \sum_{i=1}^{N} (\hat{x}_i - x_i)^2 \rightarrow \min \tag{8}$$

where *N* is the number of experimental values. This function is based on the assumption that the experimental errors are normally distributed with an average of zero.

The parameters were tested for confidence. The pseudo-confidence of each parameter interval was determined by the intersection between the axis of the parameter and the confidence surface in the case of a nonlinear model. This explains why the confidence intervals were asymmetric as we will see in the next section.

Results and Discussion

Experimental Results. A first-order kinetic law relative to toluene was assumed in order to calculate the activity and the rate of hydrogenation (r_{HYD}) in mol/(g.h). The order of reaction relative to toluene was computed in the standard conditions

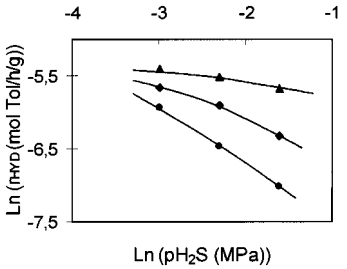

Figure 1. Hydrogenation of toluene (sulfided $NiMo/Al_2O_3$; 350 °C; H_2: 5 MPa; Toluene: 0.4 MPa; Cyclohexane: 1.4 MPa). Effect of H_2S pressure (0.05−0.2 MPa) at various partial pressure of NH_3 (▲: 0 MPa; ◆: 0.0025 MPa; ●: 0.01 MPa).

without ammonia and was found equal to 0.9 (±0.1). The toluene hydrogenation activity varied linearly with contact time. These two elements confirmed that toluene hydrogenation followed a first-order kinetics.

The effect of hydrogen partial pressure was studied between 3.0 and 6.0 MPa under 4 different H_2S partial pressures. An order of 1.2 (±0.1) with respect to hydrogen was found. The order was independent of the H_2S partial pressure.

The order of reaction relative to toluene was determined between 0.2 and 1.6 MPa. This order decreased from 1 (±0.1) to 0.4 (±0.1) when the toluene partial pressure increased. If we refer to the Langmuir−Hinshelwood theory, it means that toluene covers more and more the catalyst surface. This result confirms the first-order reaction kinetics observed at 0.4 MPa toluene partial pressure.

A complex inhibiting effect of H_2S was obtained when the H_2S partial pressure increased from 0.0125 to 1.0 MPa with a 6.0 MPa hydrogen partial pressure. The first-order kinetic constant k_{app} (s^{-1}) was determined for each H_2S partial pressure. An inhibiting effect of H_2S was found in every case, and this effect was found to be completely reversible. In fact, the order of reaction relative to H_2S decreased from −0.05 (≈0) to −0.5 as the H_2S partial pressure increased from 0.0125 to 1.0 MPa. Similar results were reported previously by Kasztelan et al.[1] in the case of a Mo/Al_2O_3 catalyst. However, although high H_2S partial pressures were reached, no evidence of a leveling off of the activity was obtained with our catalyst contrary to what was obtained with the Mo/Al_2O_3 catalyst, and we did not observe a zero order relative to H_2S at high H_2S partial pressure.

Another series of experiments was performed in the presence of ammonia generated by butylamine. The experiments showed a strong inhibiting effect of ammonia regarding the hydrogenation reaction. Even when only small amounts of ammonia were added, the catalyst activity decreased significantly. However, this strong inhibiting effect was reversible. The catalyst recovered its initial activity when ammonia was suppressed from the feed. Similar results were reported by Satterfield and Gültekin[23] concerning the hydrogenation of propylbenzene and by Chadwick et al.[24] regarding the hydrogenation of tetralin. However, Mignard et al.[25] observed that the ammonia inhibiting effect on toluene hydrogenation over a NiMo based catalyst was only partially reversible.

The effect of ammonia was studied at various H_2 (3.0, 5.0, and 6.0 MPa) and H_2S (0.05, 0.1, and 1.0 MPa) partial pressures and the results showed that the inhibition was independent of the H_2 and H_2S partial pressures. A study of the effect of the H_2S partial pressure was carried out at different ammonia partial pressures. When the ammonia partial pressure increased, the H_2S inhibiting effect was reinforced (Figure 1.). At a toluene partial pressure of 0.4 MPa and hydrogen partial pressure of 5.0 MPa, the order of reaction relative to H_2S decreased from

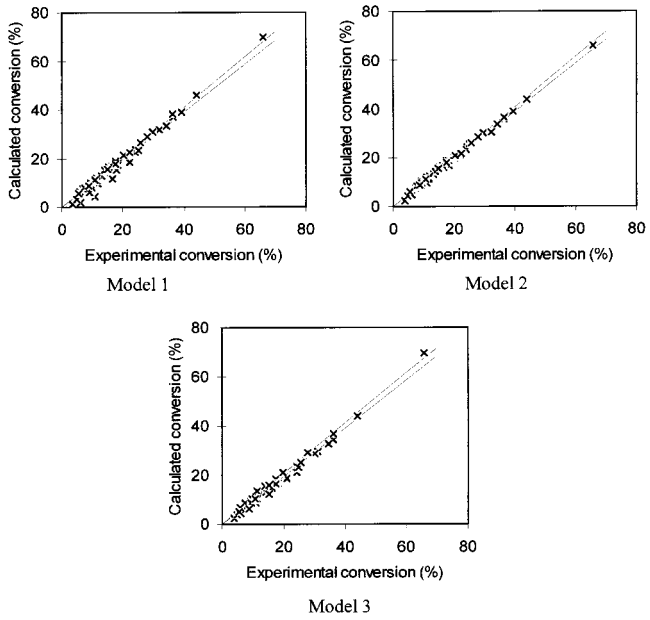

Figure 2. Hydrogenation of toluene in the absence of ammonia (sulfided $NiMo/Al_2O_3$; 350 °C). Parity diagrams. Calculated conversions versus experimental conversions.

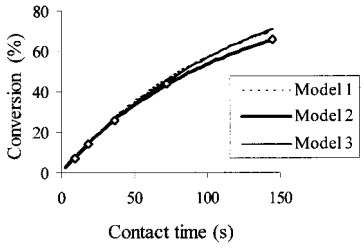

Figure 3. Hydrogenation of toluene in the absence of ammonia (sulfided $NiMo/Al_2O_3$; 350 °C; H_2: 5 MPa; Toluene: 0.4 MPa; H_2S: 0.1 MPa; Cyclohexane: 1.4 MPa). Conversion versus contact time (◇: experimental conversion).

−0.5 (±0.1) to −0.7 (±0.1) when the partial pressure of ammonia increased from 0 to 0.01 MPa. To our knowledge this unexpected effect has not yet been reported in the literature.

Kinetic Modeling. The three postulated models (see Table 1) were optimized by using the results of 45 experiments carried out in the absence of ammonia. These experiments were designed to evaluate the effect of the partial pressures of the different components (hydrogen, hydrogen sulfide, toluene, cyclohexane). The global parity diagrams show that the heterolytic models (Model 2 and 3) are more predictive than the homolytic model (Model 1), (see Figure 2). With the heterolytic models, most of the errors are smaller than the experimental errors (5%). The values of the objective function were 98 (model 1), 28 (Model 2) and 52 (Model3). The results show that the heterolytic model with the addition of the hydride first (Model 2) is apparently the best.

The effect of contact time was simulated in a range between 8 and 144 s for the three models at a H_2 partial pressure of 5.0 MPa (Figure 3). The only model which predicts the evolution of toluene conversion at high contact time correctly is the model with the hydride addition first (Model 2).

Another critical parameter to discriminate the various models is the effect of the H_2S partial pressure and particularly the dependence of the apparent kinetic constant on the H_2S partial pressure. The first-order kinetic constant was simulated for the three models and was compared with the experimental apparent

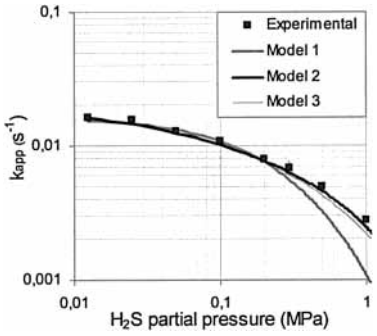

Figure 4. Hydrogenation of toluene in the absence of ammonia (sulfided $NiMo/Al_2O_3$; 350 °C; H_2: 6 MPa; Toluene: 0.4 MPa; Cyclohexane: 1.4 MPa). Evolution of the first-order kinetic constant vs H_2S partial pressure.

TABLE 2: Modeling of the Hydrogenation of Toluene in the Absence of Ammonia (sulfided $NiMo/Al_2O_3$; 350 °C; H_2: 6 MPa; Toluene: 0.4 MPa; Cyclohexane: 1.4 MPa). Model 2. Rates of the Elementary Steps (10^9 r_i) at Two Different Partial pressures of H_2S (0.0125 and 1 MPa)

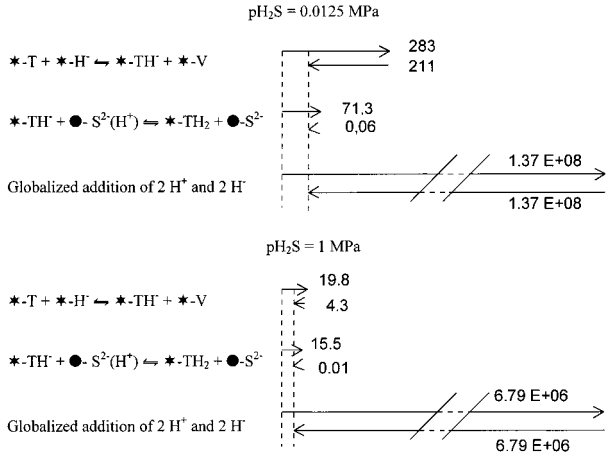

TABLE 3: Hydrogenation of Toluene in the Absence of Ammonia

parameter	value	lower limit (%)	upper limit (%)
k_1	4.98×10^{-06}	−2.21	+2.41
k_{-1}	5.47×10^{-07}	−4.02	+5.12
k_2	4.31×10^{-06}	−4.87	+4.18
k_{-2}	7.40×10^{-14}	−23.51	+63.51
B_{H_2}	1.17×10^{-03}	−2.56	+2.56
B_{H_2S}	424	−7.55	+6.84
$b_{toluene}$	3110	−2.89	+2.89
b_{MCH}	48	−100	+2800
b_{CHX}	1410	−7.80	+7.80

Estimated parameters (Model 2) and their confidence interval (%).

kinetic constants (Figure 4). The heterolytic models are again more predictive than the homolytic model at high H_2S partial pressure. The heterolytic model with the hydride addition first (Model 2) seems to represent the effect of H_2S better than the heterolytic model with the proton addition first (Model 3).

The interest of the CHEMKIN/SURFACE-CHEMKIN II approach is that it offers the possibility to obtain the values of the rates of the elementary steps for every given contact time conveniently. Table 3 gives the rates of the direct and reverse elementary steps for the hydrogenation of toluene in the case of Model 2. This presentation makes it possible to visualize the differences in reaction rates under two different H_2S partial pressures. We can notice that the rate-determining step is the

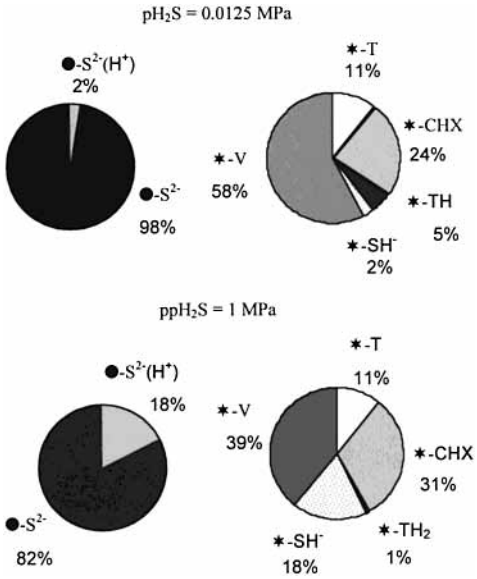

Figure 5. Hydrogenation of toluene in the absence of ammonia (sulfided $NiMo/Al_2O_3$; 350 °C; H_2: 6 MPa; Toluene: 0.4 MPa; Cyclohexane: 1.4 MPa). Changes of surface coverage at 0.0125 and 1.0 MPa of H_2S partial pressure.

addition of a proton on the partially hydrogenated intermediate but the limiting character of the addition of the proton decreases in importance when the H_2S partial pressure increases. This can be explained by considering the surface coverage which can be calculated by the model (Figure 5). At low H_2S partial pressure, the surface coverage by protons is low, justifying that the proton addition is clearly the rate-determining step. When the H_2S partial pressure increases, the surface coverage by protons increases. This increase is due to the heterolytic dissociation of H_2S which produces protons.[26] The increase of the surface coverage by protons between 0.0125 and 1.0 MPa H_2S partial pressure has a enhancing effect on the rate of the proton addition. Moreover, the heterolytic dissociation of H_2S leads also to the formation of sulfhydril ions adsorbed on coordinatively unsaturated Mo ions. This induces an inhibiting effect on the hydride addition step. In fact, sulfhydril species compete with hydride ions for the adsorption on the coordinatively unsaturated Mo ions. The surface coverage by hydrides is four times lower at 1.0 MPa than at 0.0125 MPa H_2S partial pressure ($7\ 10^{-6}$ vs $3\ 10^{-5}$). It is worth noting that the hydride surface coverage is lower than the coverage with other species. However, the surface coverage by toluene is independent of the H_2S partial pressure, probably because of the high value of the toluene adsorption/desorption constant compared with the H_2S adsorption/desorption constant (Table 3). Globally, H_2S has an inhibiting effect by decreasing the hydride species concentration on the catalyst surface as well as that of the partially hydrogenated intermediate (✶-TH^-). The decrease in the concentration of the TH^- species leads to a decrease in the rate of the proton addition, which is the rate-limiting step, and consequently to a decrease of the hydrogenation rate. However the inhibiting effect of H_2S is more significant at high than at low partial pressure. This is the consequence of the dual character of H_2S, both promoting by producing protons and inhibiting through its competition toward adsorption with the species involved in the rate-determining step. At low partial pressures of H_2S where the addition of the proton is highly rate-limiting the inhibiting effect due to the adsorption is greatly compensated by the kinetic effect, which means that the resulting inhibiting effect of H_2S is quite limited. At higher partial pressures of H_2S, the compensation effect is much more

TABLE 4: Hydrogenation of Toluene in the Presence of Ammonia

model 2A	value	lower limit (%)	upper limit (%)
k_1	1.53×10^{-02}	−2.61	7.84
k_{-1}	1.29×10^{-08}	−33.57	20.93
k_2	1.26×10^{-07}	−16.67	51.59
k_{-2}	1.39×10^{-13}	−13.67	111.51
B_{H_2}	4.79×10^{-06}	−1.67	5.64
B_{H_2S}	$6.1 \times 10^{+03}$	−10.07	2.96
b_{NH_3}	$4.44 \times 10^{+05}$	−9.91	4.73
$b_{toluene}$	467	−2.57	7.92
$b_{methylcyclohexane}$	0.10	−100	10^{+06}
$b_{cyclohexane}$	49.6	−100	2360

model 2B	value	lower limit (%)	upper limit (%)
k_1	1.11	−1.80	7.21
k_{-1}	2.26×10^{-04}	−7.08	2.22
k_2	2.48×10^{-06}	−2.02	7.66
k_{-2}	2.6×10^{-14}	−11.54	91.16
B_{H_2}	1.22×10^{-06}	−0.82	5.74
B_{H_2S}	$2.94 \times 10^{+04}$	−8.81	2.57
B_{NH_4}	$2.32 \times 10^{+06}$	−1.72	1.29
$b_{toluene}$	$1.01 \times 10^{+03}$	−2.08	7.92
$b_{methylcyclohexane}$	1.24	−100	10^{+06}
$b_{cyclohexane}$	162	−100	77.78

Estimated parameters and their confidence interval (%).

limited and, consequently the resulting inhibiting effect of H_2S is more pronounced.

It must be added that in a previous study[1] it was found by using a Langmuir−Hinschelwood approach that the rate-limiting step of the hydrogenation of toluene on a MoS_2/Al_2O_3 catalyst was the hydride addition at low H_2S partial pressure and the proton addition at high H_2S partial pressure, which is not in accordance with the present results. Apart from the fact that it was not the same catalyst, this discrepancy can be attributed to the fact that with the CHEMKIN method we have not to make all the assumptions which are necessary in the case of Langmuir-Hinschelwood models, particularly the assumptions concerning the adsorption strength of the reactants. In principle this should make the CHEMKIN method more reliable.

In the case of Model 2, the parameters were tested for confidence. The confidence intervals are reported in Table 3. The results show that the methylcylohexane adsorption/desorption constant is not sensitive. This might be due to the fact that in our experimental conditions the dehydrogenation reaction of methylcyclohexane was disfavored and that the methylcyclohexane coverage was very low in comparison with the toluene and cyclohexane surface coverage. We can assume that the wide confidence interval for parameter k_{-2} is due to the very low value of the parameter compared with the others.

Regarding the experiments in the presence of ammonia, the models were optimized by using the results of 44 experiments corresponding to the variations of H_2, H_2S, and ammonia partial pressures. The objective function values show that the heterolytic models (Model 2A and 2B) are more predictive than the homolytic model (Model 1A). The values were 17 in the case of the heterolytic models and 25 in the case of the homolytic model. However, it is completely impossible to discriminate between the possible adsorption modes of ammonia (coordination or protonation). Parity diagrams do not give significant elements to differentiate these two models.

The parameters for models 2A and 2B and their confidence intervals are reported in Table 4. Like in the absence of ammonia, the methylcyclohexane adsorption constant is not sensitive, certainly for the same reasons. It is worth noting that for the two models 2A and 2B, the H_2S adsorption/desorption constant is higher in the presence of ammonia than in its absence (compare B_{H_2S} in Table 3 and Table 4), which is in line with the fact that the inhibiting effect of H_2S was found greater in the presence of ammonia than in its absence. In fact, it was impossible to reconcile the models for the reactions in the presence of ammonia with those corresponding to the experiments in the absence of ammonia. This can be explained either by a coupling interaction between H_2S and NH_3 on the surface or by a modification of the catalyst surface due to the presence of ammonia.

Actually, in the particular case of model 2B, NH_3 can stabilize the protons resulting from the dissociation of H_2S by forming adsorbed ammonium ions hence enhancing the inhibiting effect of H_2S

$$H_2S + ✱\text{-}V + ●{-}S^{2-} \rightleftharpoons ✱\text{-}SH^- + ●\text{-}\ S^{2-}(H^+)$$

$$NH_3 + ●\text{-}\ S^{2-}(H^+) \rightleftharpoons ●{-}S^{2-}(NH_4^+)$$

The idea is that the adsorption strength of NH_4^+ resulting from the protonation of ammonia by an adsorbed proton issuing from H_2S is greater than the adsorption strength of a proton (issuing from H_2S) simply adsorbed on a sulfide anion of the catalyst. In other words, the combination of the adsorptions of H_2S and of NH_3 reinforces that of the former by stabilizing the proton. The consequence is a displacement of the equilibrium of adsorption of H_2S in favor of the adsorbed state, which means an increase of the adsorption constant of H_2S (B_{H_2S}).

It was found previously that on sulfided catalysts treated with ammonia[27] as well as on aged catalysts,[28] certain nitrogen species were strongly attached to the catalyst. Hence, a possible explanation for the fact that different sets of parameters are necessary to account for the results with and without ammonia is that the adsorption of ammonia could induce electronic modifications of the active sites which would not be taken into account by the kinetic modeling.

Actually, the analysis of the surface coverage by adsorbed species show that the ammonia either coordinatively adsorbed (Model 2A) or protonated (Model 2B) occupies a large fraction of the surface. This corresponds to a high value of the ammonia adsorption/desorption constant compared with those of the other species (Table 4).

Like in the absence of ammonia, the rate-determining step is still the addition of the proton to the partially hydrogenated intermediate (✱-TH^-).

Conclusion

The kinetic modeling of the effect of H_2S and of NH_3 on toluene hydrogenation reported in this work allowed us to discriminate between different possible mechanisms. It brings new elements in favor of the heterolytic dissociation of H_2 and H_2S on sulfided $NiMo/Al_2O_3$ hydrotreating catalysts. The toluene hydrogenation mechanism starting with a hydride addition followed by a proton addition is more predictive than a heterolytic mechanism with a reverse sequence or a homolytic mechanism. In particular, it accounts very well for the effect of the H_2S partial pressure. However, the rate-determining step is the proton addition on the partially hydrogenated intermediate. For the experiments in the presence of ammonia, the model corresponding to the heterolytic dissociation with the addition of the hydride first was also the most predictive. However, it was not possible to discriminate between the possible modes

of ammonia adsorption. Moreover, it was not possible to reconcile the models for the reaction in the presence of ammonia with those in the absence of ammonia. This can be due to a modification of the surface or to an interaction between hydrogen sulfide and ammonia as shown by the fact that hydrogen sulfide was more strongly adsorbed in the presence of ammonia than in its absence thus enhancing the inhibiting effect of H_2S on toluene hydrogenation.

The approach used in this work has two major advantages. First, the use of CHEMKIN/SURFACE CHEMKIN II does not require to make assumption on the rate-determining step as in the case of a Langmuir−Hinshelwood approach; second, it gives access to the surface coverage by the various species and to the direct and reverse rates of each elementary step.

Acknowledgment. S. Blanchin wishes to thank IFP for a Ph. T. fellowship.

Symbols

Y_k: weight fraction of component k
t_c: contact time
A: BET surface area (m^2/g)
w_k: molecular weight of component k(g/mol)
ρ_c: catalyst density (g/cm^3)
ρ: gas-phase density (g/cm^3)
$\dot{S}_k$: production-destruction rate of species k ($mol/cm^2 \cdot s$)
n_g: number of gas-phase species
Z_k^n: fraction of site of type n covered by species k
Z_s^n: fraction of uncovered site of type n
C_k^{gas}: concentration of species k in the gas phase
$m(n)$: number of species adsorbed on the site of type n
b_k, B_k: adsorption/desorption constants (cm^3/mol)
K_p: thermodynamic equilibrium constant of toluene hydrogenation
k_i: kinetic constant of the elementary steps
P: total pressure
T: temperature
S: least-squares functions
x_i: experimental conversion
$\hat{x}_i$: calculated conversion

References and Notes

(1) Kasztelan, S.; Guillaume, D. *Ind. Eng. Chem. Res.* **1994**, *33*, 203.
(2) Girgis, M. J.; Gates, B. C. *Ind. Eng. Chem. Res.* **1991**, *30*, 2021.
(3) Pérot, G. *Catal. Today* **1991**, *10*, 447.
(4) Coccheto, J. F.; Satterfield, C. N. *Ind. Eng. Chem. Process. Des. Dev.* **1981**, *20* (1), 53.
(5) Vivier, L.; D'Araujo, P.; Kasztelan, S.; Pérot, G. *Bull. Soc. Chim. Belg.* **1991**, *100* (11−12), 801.
(6) Kasztelan, S.; Wambeke, A.; Jalowiecki, L.; Grimblot, J.; Bonnelle, J. P. *Bull. Soc. Chim. Belg.* **1987**, *96*, 1003.
(7) Komatsu, T.; Hall, W. K. *J. Phys. Chem.* **1991**, *95*, 9966.
(8) Tanaka, K.; Okuhara, T. *Catal. Rev.-Sci. Eng.* **1977**, *15*, 249.
(9) Tanaka, K. *Adv. Catal.* **1985**, *33*, 99.
(10) Thomas, C.; Vivier, L.; Lemberton, J. L.; Kasztelan, S.; Pérot, G. *J. Catal.* **1997**, *167*, 1.
(11) Wambeke, A.; Jalowiecki, L.; Kasztelan, S.; Grimblot, J.; Bonnelle, J. P. *J. Catal.* **1988**, *109*, 309.
(12) Lacroix, M.; Yuan, S.; Breysse, M.; Dorémieux-Morin, C.; Fraissard, J. *J. Catal.* **1992**, *138*, 409.
(13) Jobic, H.; Clugnet, G.; Lacroix, M.; Yuan, S.; Mirodatos, C.; Breysse, M. *J. Am. Chem. Soc.* **1993**, *115*, 3654.
(14) Anderson, A. B.; Al-Saigh, Z. Y.; Hall, W. K. *J. Phys. Chem.* **1988**, *92*, 803.
(15) Le Page, Catalyse de Contact, Eds Technip, Paris, **1978**.
(16) Kee, R. J.; Rupley, F. M.; Miller, J. A., "Chemkin-II: a Fortran Chemical Kinetics Code Package for the Analysis of Gas-Phase Chemical Kinetics", SANDIA National Laboratories Reports, Livermore, **1989**, SAND89-8209.
(17) Coltrin, M. E.; Kee; R. J.; Rupley, F. M. "Surface Chemkin (Version 4.0): A Fortran Package for Analyzing Heterogeneous Chemical Kinetics at a Solid-Surface−Gas-Phase Interface", SANDIA National Laboratories Reports, Livermore, **1991** Rept. SAND90-8003B.
(18) Petzold, L. R. "A description of DASSL: a Differential/Algebraic System Solver", Applied Math Division., SANDIA National Laboratories Reports, Livermore, **1989** Rept. SAND82-8367.
(19) Gear, C. W. *IEEE Trans. on Circuit Theory*, *CT-18* **1971**, *1*, 89.
(20) Kasztelan, S. *Hydrotreating Technology for Pollution Control. Catalysts, Catalysis and Processes*, Chemical Industries, Occelli, M. L., Chianelli, R., Eds, Marcel Dekker: New York, Hong Kong, 1995, vol. 67, p 29.
(21) Kasztelan, S. *Ind. Eng. Chem. Res.* **1992**, *31*, 2497.
(22) Abadie, J. *The GRG Method for Nonlinear Progamming, Design and Implementation of Optimization Software*. H. J. Greenberg, Sijthoff and Nordhoff, Alphen aan den Rijn, Netherlands, **1978**, 335.
(23) Satterfield C. N.; Gültekin, S. *Ind. Eng. Chem. Process Des. Dev.* **1984**, *23*, 179.
(24) Chadwick, D.; Oen, A.; Siewe, C. *Catal. Today* **1996**, *29*, 229.
(25) Mignard, S.; Marchal, N.; Kasztelan, S. *Bull. Soc. Chim. Belg.* **1995**, *104*, 259.
(26) Topsoe, N. Y.; Topsoe, H. *J. Catal.* **1993**, *139*, 641.
(27) Zeuthen, P.; Blom, P.; Muegge, B.; Massoth, F. E. *Appl. Catal.* **1991**, *68*, 117.
(28) Zeuthen, P.; Blom, P.; Massoth., F. E. *Appl. Catal.* **1991**, *78*, 265.